On the effective medium theory of subwavelength periodic structures

PHILIPPE LALANNE

Institut d'Optique Théorique et Appliquée, CNRS, URA 14, BP 147, 91403 Orsay Cedex, France

DOMINIQUE LEMERCIER-LALANNE Lycée Janson de Sailly, 75015 Paris, France

(Received 25 May 1995; revision received 10 October 1995)

Abstract. The effective medium theory of one-dimensional and two-dimensional periodic structures are investigated. A method based on a Fourier decomposition of the wave propagating along the direction perpendicular to the periodic structures allows one to determine the zeroth-, first- and second-order effective indices. For one-dimensional problems, we derive closed-form expressions of the effective indices for both TE and TM polarization. Our result can be applied to arbitrary periodic structure with symmetric or non-symmetric lamellar or continuously varying index profiles. The theoretical predictions are carefully validated using rigorous coupled-wave analysis. For the two-dimensional case, only symmetric structures are discussed and the computation of the zeroth-, first-, and second-order effective indices requires the inversion of an infinite matrix which can be truncated and simply solved numerically. The EMT prediction is qualitatively validated using rigorous computation for small period-to-wavelength ratios. It is shown that for large period-to-wavelength ratios near the cutoff value, no analogy between 2-D periodic structures and homogeneous media holds for highly modulated lamellar gratings.

1. Introduction

Recent experimental and theoretical investigations have shown that periodic subwavelength structured surfaces with periods which are small compared to the illumination wavelength behave as homogeneous media and have suggested interesting applications, such as fabrication of anti-reflection coatings [1-6], quarter wave plates [7, 8], polarizers [9], and graded-phase diffractive elements [10-12]. The replacement of the periodic structure by a homogeneous medium is often referred to as homogenization or effective medium theory (EMT). EMT can be applied to a large variety of physical material properties [13], such as the diffusion constant, magnetic permeability, thermal conductivity, etc. To facilitate the design and fabrication of artificial dielectric elements, one must be able to relate the effective index of the subwavelength structured surface in a simple way. The properties of one-dimensional (1-D) periodic structures have been analysed in great detail, and the equivalence of 1-D gratings and homogeneous uniaxial thin films has been rigorously derived in the long wavelength limit. Throughout the paper, the long wavelength limit refers to infinitely small periods compared to the wavelength illumination and corresponds to zeroth-order static EMT solutions. A closed-form EMT solution for 1-D periodic lamellar structures composed of two homogeneous materials was derived by Rytov [14]. By matching Maxwell's boundary conditions inside the periodic structure, he found the three effective indices for wave propagation along the lamellar stack with the electric field parallel to the grating vector (TM polarization) or perpendicular to the grating vector (TE polarization), and for waves propagating perpendicularly to the lamellar stack. Rytov's approach which is based on matching the boundary conditions inside the periodic structure can be referred to as a modal approach. Using a more rigorous modal formalism, MacPhedran et al. [15] studied the long wavelength limit of 1-D lossy lamellar gratings and showed that the equations of electrostatic can be used to rigorously determine the zeroth-order effective index. By using a Fourier expansion wave basis of the field inside the periodic structure, Bell et al. [16] generalized these previous works to an arbitrary 1-D symmetric profile. They showed that symmetric gratings are equivalent to an uniaxial film in the long wavelength limit, and derived a closed-form for the second-order effective index of symmetric 1-D gratings and for TE polarization. Bouchitte and Petit [17] provided a rigorous demonstration of the equivalence of 1-D gratings and thin films in the long wavelength limit. Haggans et al. [18] studied the EMT of 1-D lamellar periodic structures in conical mountings, and Campbell and Kostuk [19] modelled sinusoidally modulated and slanted gratings for conical and non-conical mountings.

Limited research has been done in the area of two-dimensional (2-D) gratings. Jackson and Coriell [20] derived upper and lower bounds of the zeroth-order effective index of 2-D periodic structures. Their work was mainly motivated by the derivation of transport coefficients of materials composed of two different homogeneous media, but can be applied to optical coefficients such as the magnetic permeability or the dielectric constant. Because these bounds are generally quite narrow when the two media have similar optical indices, their average represents a good approximation of the zeroth-order effective index [12, 13]. Motamedi et al. [5] proposed an approximate solution for the zeroth-order effective index by averaging the two zeroth-order TM and TE effective indices of 1-D gratings. As was noted by Grann et al. [21], Motamedi's solution is strongly inaccurate. By making an analogy from the series and parallel equivalent circuit model, Brauer and Bryngdahl [22] proposed a more accurate formula. In fact, their EMT solution is a weighted average of three indices, the upper and lower bounds derived in [13] and the average index of the periodic structure. More recently, Grann et al. [21] used rigorous coupled-wave analysis (RCWA) to estimate the effective index of 2-D gratings by computer simulations.

In this paper we study the EMT of 1-D and 2-D periodic structures for a wave propagating normally to the grating. We use the Fourier expansion method proposed by Bell et al. [16]. In particular for TE polarization and 1-D structures, we provide simulation results showing that their approach is not restricted to symmetric structures. For TM polarization and 1-D structures, we derive a closed-form of the second-order effective index. For 2-D symmetric periodic structures, closed-forms of the zeroth- and second-order effective indices are provided. By 2-D symmetric structures, we mean structures presenting a centre of symmetry. It does not imply that the periods are the same, and for gratings composed of parallelipipeds of one given medium immersed in another medium, it does not imply that the two fill factors are equal. To our knowledge, this work is the first to derive the second-order effective index of arbitrary 1-D periodic structures with TM polarization, and to present a rigorous approach for the EMT of 2-D period structures.

In our approach, the EMT is derived by considering the propagation of a periodic wave with a plane-wave dependence along the direction of propagation. The periodic structure is assumed to have an infinite spatial extent in all the directions. To verify the EMT predictions, a finite spatial extent of the periodic structure is inserted between two semi-infinite homogeneous media. This defined a grating diffraction problem which is solved by rigorous computation. We then verify the effective index predictions by comparing the transmitted and reflected amplitudes obtained with rigorous computation and with a homogeneous thin film whose optical index is equal to the EMT prediction. In this comparison, the thickness of the grating and that of the thin film are assumed to be equal. As was noted by Grann and Moharam [23], the effective properties of subwavelength gratings cannot be simply described by an effective index. When the grating thickness is much smaller than the wavelength, they showed that an effective thickness has to be introduced to accurately describe the effective properties. In our experience, the effective thickness must not be taken into account for a grating thickness larger than about one tenth of a wavelength. In this paper, this effect is not discussed and the grating thickness chosen for comparison is much larger than the critical value of one tenth of wavelength. Consequently, this paper is devoted to the study of wave propagation in media with periodic permittivity, and not to the equivalence between subwavelength periodic structures and homogeneous thin films. This is the reason why, in order to avoid any confusion in the following, we prefer to refer to EMT rather than to homogenization.

In section 2, we first introduce the notation and present the methodology used throughout the paper. The methodology is basically the same as those provided in [16], except that the EMT solution is derived without expanding the field in a power series of the period-to-wavelength ratio. As was pointed out in [17], the existence of such power series would require more study. In section 2.2, we solve the problem of 1-D periodic structures for TE polarization. In section 2.3 using RCWA simulations, we emphasize that the EMT solution is valid even for non-symmetric gratings. Section 3 is related to the EMT of 1-D periodic structures for TM polarization. A closed-form of the zeroth- and second-order effective indices is first derived. When applied to lamellar periodic structures composed of two alternate layers, the closed-form is shown to be identical to a previous result obtained by Rytov [14]. Then using RCWA simulations, the generality of our EMT solution is tested for continuously varying index profiles. In section 4, the EMT of 2-D symmetric periodic structures is derived. The calculus is more complex but the methodology remains the same. A closed-form of the zeroth- and second-order effective indices is derived for symmetric gratings. The long wavelength limit effective index is shown to lie in between the upper and lower bounds of [13], and the second-order effective index formula is tested by RCWA. Section 5 concludes and summarizes the results of the paper.

Methodology and EMT of one-dimensional structures for TE polarization

To establish our notation, let us first consider a 1-D periodic structure along the y axis with an arbitrary relative permittivity profile $\varepsilon(y)$, as shown in figure 1. The structure is assumed to be constant in the x and z directions. The grating period along the y direction is denoted as Λ , and the grating-vector module K is simply defined as $K = 2\pi/\Lambda$. When considering 2-D periodic structures, the relative

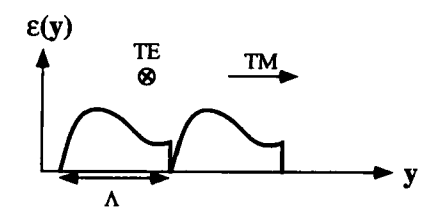


Figure 1. 1-D periodic structure along the y axis. The relative permittivity is independent of x and z coordinates. Λ denotes the period. TE and TM polarization correspond to electric fields parallel to the x and y directions, respectively.

permittivity $\varepsilon(x,y)$ depends on both x and y coordindates and is constant in the z-direction. Again Λ denotes the period along the y direction. The period in the x direction Λ_x can be simply written as $\Lambda_x = \Lambda/\rho$, where ρ is a dimensionless coefficient. Again we note $\mathbf{K} = 2\pi/\Lambda$. For both 1-D and 2-D structures, Λ and \mathbf{K} are related to the periodicity along the y direction. Using ε_{mn} to denote the (m, n)th Fourier coefficient of period structures, we have

$$\varepsilon(x, y) = \sum_{m, n} \varepsilon_{m, n} \exp iK(\rho mx + ny). \tag{1}$$

Similarly, for 1-D structures, we have

$$\varepsilon(y) = \sum_{m} \varepsilon_{m} \exp iKmy.$$
 (2)

Also, we denote the Fourier coefficients of $1/\varepsilon(x, y)$ and $1/\varepsilon(y)$ by $a_{m,n}$ and a_m , respectively. Magnetic effects are not considered in this paper so that the permeability of periodic structures is constant and noted μ_0 everywhere.

2.1. Methodology

For both 1-D and 2-D periodic structures, we will consider a wave with wavelength λ in the vacuum and wave-module vector \mathbf{k} ($\mathbf{k} = 2\pi/\lambda$). The wave is propagating in the periodic structure along the z direction and is polarized in either the x or y direction. Note that because of the symmetry degeneracy of 1-D periodic structures, the z and x directions are equivalent. A temporal dependence $\exp(-i\omega t)$ is assumed for the wave. For 1-D (resp. 2-D) gratings, we assume that the wave amplitude is periodic in the y (resp. x and y) direction. The z-dependence of the wave amplitude is given by

$$\exp\left(\mathrm{i}(\eta)^{1/2}\mathbf{k}z\right). \tag{3}$$

The constant η is read as the square of the effective index of the periodic structures for the z direction and the given polarization. Then the periodic wave with the z-dependence of equation (3), is used in satisfying Maxwell's equations inside the periodic structure. Obviously such a solution is not correct, but we will see that, at least for small period-to-wavelength ratios, it is possible to find a particular η value such that Maxwell's equations are satisfied. As only the limit of small period-to-wavelength ratios are considered in the following, it is convenient to expand η in a power series of $\alpha = \lambda/\Lambda$

$$\eta = \eta_0 + \eta_1 \alpha^{-1} + \eta_2 \alpha^{-2} + \cdots,$$
(4)

where η_0 is the square of the zeroth-order effective index and η_i , i = 1, ..., N is the *i*th-order coefficient of the series expansion. In general η depends on the permittivity ε , the period Λ , the wavelength λ , and on ρ for 2-D periodic structures. In the literature, the zeroth-order EMT is also referred to as the quasi-static limit or the long wavelength limit. Note that the above methodology is strictly the same as in [16]. It is used for the 1-D TE and TM problems, and for the 2-D problems.

2.2. EMT of one-dimensional structures: TE polarization

We look for a wave propagating in the z direction and periodic in the y direction with period Λ . The x component of the electric field denoted A(y, z) can thus be expanded as a Fourier series and according to equation (3), can be written

$$A(y,z) = \exp\left(i(\eta)^{1/2} \mathbf{k}z\right) \sum_{m} A_{m} \exp\left(i\mathbf{K} m y\right), \tag{5}$$

where A_m is a constant coefficient. To satisfy Maxwell's equations, the wave of equation (5) must simply satisfy Helmholtz's equation $\Delta A + \mathbf{k}^2 \varepsilon(y) A = 0$. By identifying in the plane-wave basis, we find the infinite set of linear equations

$$\forall i, \quad (\varepsilon_0 - i^2 \alpha^2 - \eta) A_i + \sum_{p \neq i} \varepsilon_{i-p} A_p = 0. \tag{6}$$

By looking for a nontrivial solution of this homogeneous system, the effective permittivity η is seen as the value which obeys the dispersion relation

For a $(2N+1)\times(2N+1)$ determinant, equation (7) can be read as the nullity of a polynomial in α^2 of degree 2N. Substituting the asymptotic series from equation (4) into the determinant, it is straightforward to derive that $\eta_0 = \varepsilon_0$ so that the highest order α^{4N} of the polynomial equals zero. It is also easy to show that for any i, $\eta_{2i+1} = 0$. Elementary algebraic manipulations show that by annulling the coefficient of order 4N-2 in the determinant, the expression of η_2 is derived. Finally, we obtain

$$\eta = \varepsilon_0 + \alpha^{-2} \sum_{p \neq 0} \frac{\varepsilon_{-p} \varepsilon_p}{p^2} + O(\alpha^{-4}). \tag{8}$$

Equation (8) is the same as equation (15) of the paper by Bell and his co-workers [16]. To derive equation (8), these authors expanded the diffracted wave amplitudes

 A_i in a power series of α^{-1} , and restricted their discussion to symmetric grating profiles. We emphasize here that equation 8 can also be applied to non-symmetric structures, since it was derived without any restriction on the periodic structure profile. The next section provides computational evidence with a non-symmetric example. In [17], Bouchitte and Petit noted that the power series expansion used by the authors of [16] was a point of concern in their mathematical approach, and that the validity of expansion would require more in-depth studies. Our demonstration simply employs a power series expansion for the relative effective permittivity of equation (4), and not for the diffracted wave amplitudes A_i . The fact that our derivation and that of [16] gives the same EMT result makes firmer our opinion that the series expansion of A_i is valid. Note, however, that this concordance does not really demonstrate the validity of the series expansion. In fact, it is our opinion that the series expansion of A_i is provides a convenient way to simply derive equation (8), and even to obtain higher order terms in α^{-4} , α^{-6} , etc. It will be used in section 4.4 to derive the second-order effective index of 2-D symmetric periodic structures.

2.3. Simulation results

In order to verify the behaviour with α of the effective index given by equation (8), we proceed as follows. First, we choose the non-symmetric periodic structure shown in figure 2. Each layer is homogeneous with relative permittivity $\varepsilon_{\rm I}=1$ and $\varepsilon_{\rm II}=16$. Parameters a,b,c and d define the position of the layer boundaries. Their numerical values are given in the caption of figure 2. We choose a non-symmetric grating in order to test the validity of equation (8) for non-symmetric structures. Then we insert a finite section of this structure between two semi-infinite homogeneous regions of permittivities $\varepsilon_{\rm I}$ and $\varepsilon_{\rm II}$, respectively. The depth h of the periodic structure was taken to be equal to four wavelengths in the simulations. Figure 2 defines a diffraction problem that we solve using RCWA for an incident plane wave of unit amplitude, normally incident from the region of relative permittivity $\varepsilon_{\rm I}$. Solving Maxwell's equations, we compute the complex transmitted amplitude t and reflected amplitude t of the zeroth-order diffracted waves. Then making the analogy between subwavelength periodic structures and a homogeneous medium, we define the equivalent effective index of the periodic structure by the

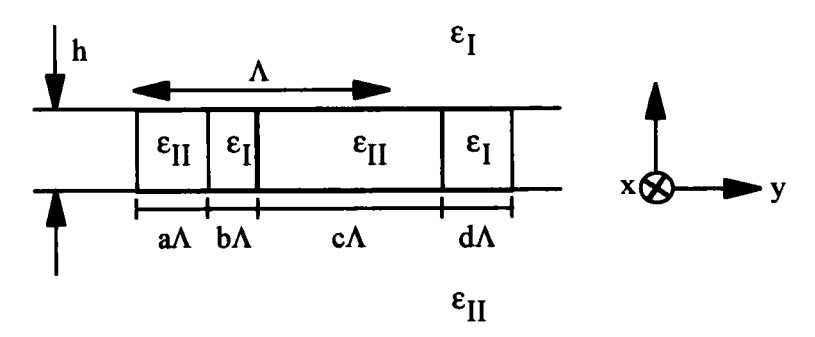


Figure 2. TE polarization case. Non-symmetric periodic structure of depth h inserted between two homogeneous regions of permittivities $\varepsilon_{\rm I}=1$ and $\varepsilon_{\rm II}=16$. The periodic structure is composed of alternate layers of permittivities $\varepsilon_{\rm I}$ and $\varepsilon_{\rm II}$, and is defined by the transition walls a=0.1, b=0.2, c=0.6 and d=0.1. $h=4~\mu{\rm m}$ and $\lambda=1~\mu{\rm m}$ were chosen for the computation.

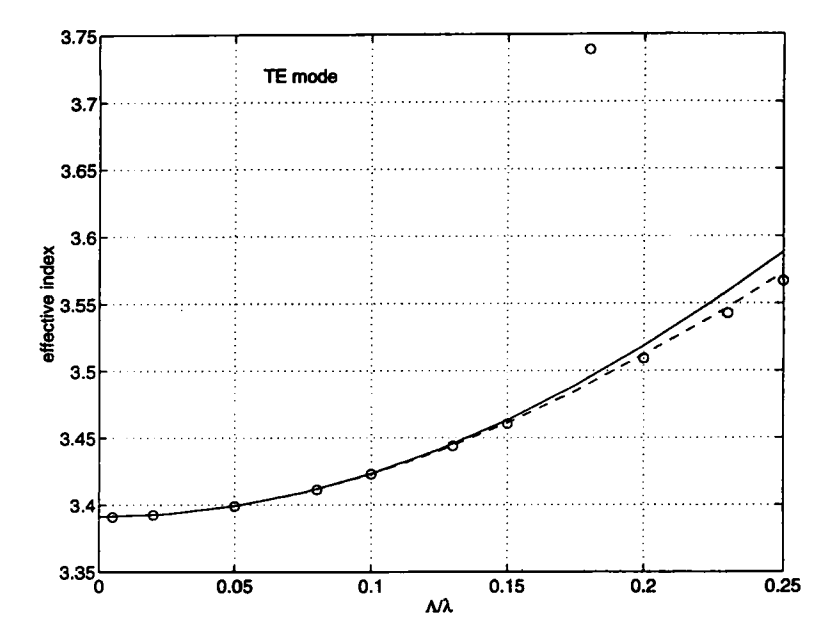


Figure 3. Simulation results for TE polarization. The solid curve represents the effective index of equation (8) when applied to the grating problem of figure 2. The circle-marks are the effective indices n_{RCWA} obtained by minimizing the error function of equation (9). 201 orders were retained for the RCWA computation. The dashed curve corresponds to the effective index prediction when the α^{-4} term in the series expansion of equation (8) is included.

real number n_{RCWA} which minimizes the error function

$$e = |r'(n_{\text{RCWA}}) - r|^2 + |t'(n_{\text{RCWA}}) - t|^2,$$
 (9)

where $r'(n_{\text{RCWA}})$ and $t'(n_{\text{RCWA}})$ are the reflection and transmission complex coefficients of a thin homogeneous layer of thickness h and optical index n_{RCWA} , inserted between two infinite media of relative permittivities ε_{I} and ε_{II} . The effective index n_{RCWA} is supposed to be larger than the minimal value of the grating index, and smaller than the maximal value of the grating index. For example, for the grating of figure 2, $n_{\text{RCWA}} \in [(\varepsilon_{\text{I}})^{1/2}; (\varepsilon_{\text{II}})^{1/2}]$.

Figure 3 provides a comparison between the EMT prediction of equation (8) and those of RCWA. The comparison is made over the complete operating region of the grating defined in figure 2 as a zeroth-order filter. The solid line corresponds to the effective index of equation (8). The 11 circle-marks correspond to the effective indices n_{RCWA} computed with RCWA and by minimizing the error function of equation (9). The maximum error, e, obtained with the 11 RCWA computations was 0.058. This value is an important feature of the comparison, since it quantifies the confidence someone can expect in the EMT prediction. For example, the error e of 0.058 corresponds to a difference in reflected intensity $|r'(n_{\text{RCWA}})|^2 - |r|^2$ of 0.029, which is less than 3%. In general, the error e increases with the parameter α . This is not surprising as one would expect that the EMT predictions are more accurate for small period-to-wavelength ratios. In figure 3, the maximum error (e = 0.029) is obtained for the largest value of α ,

namely $\alpha=0.25$. We first conclude that there is an excellent matching between the theoretical prediction and simulation results, even for large values of Λ/λ that reach the upper bound $1/(\epsilon_{\rm II})^{1/2}$, beyond which the grating of figure 2 stops behaving as a zeroth-order filter for normal incidence. We note that the effective index prediction including the α^{-4} correction term (shown on the dotted line in figure 3) provides still better agreement with rigorous computations.

For $\alpha = 0.18$, the circle-mark differs greatly from the value 3.49 predicted by equation (8). An effective index of 3.49 gives an error function e = 0.023 and a difference in reflected intensity of 9.2×10^{-5} . The effective index, $n_{RCWA} = 3.74$, obtained with RCWA gives a lower error e = 0.0031 and a slightly higher difference in reflected intensity of 3.4×10^{-4} . This shows that the computation defined by the minimization of the error function of equation (9) is not wellconditioned: even if only one absolute minimum in the considered interval exists, there are in general several good potential candidates for n_{RCWA} . Two comments have to be made in relation with the ill-conditioning. Firstly, since small variations of the transmitted and reflected amplitudes computed with RCWA can induce large variations of the effective index n_{RCWA} , RCWA convergence has to be guaranteed. In figure 3, 201 orders were retained for the computation. This was largely sufficient since the same results were obtained with 101 retained orders. However, we note that for 51 retained orders, significantly different n_{RCWA} results were obtained. Secondly, the error criterion of equation (9) is somewhat arbitrary. For instance, in [21], the authors used two other different criteria depending only on the comparison of the reflected intensities. This was probably due to the fact that these authors were mainly concerned by the anti-reflection properties of subwavelength gratings. However, it it our opinion that the criterion of equation (9) is worth considering, as it takes into account both reflected and transmitted waves in the analogy. Only this criterion will be used in the following. As a matter of fact, the discrepancy observed in figure 3 for $\alpha = 0.18$ has to be attributed to an artefact resulting from the chosen criterion and to the only approximate analogy between subwavelength gratings and homogeneous thin films. The error e = 0.023 obtained with the effective index n = 3.49 is an acceptable value equal to the one obtained for $\alpha = 0.25$ and comparable to those obtained for $\alpha = 0.2$ and 0.23. So we conclude that the EMT prediction of equation (8) has been validated over the complete operating region of the grating of figure 2 as a zeroth-order filter.

EMT of one-dimensional structures: TM polarization

3.1. Derivation of the effective relative permittivity

Let us now suppose a wave propagation in the z direction and polarized in the x direction. The magnetic field A(y, z) is parallel to the x direction and is given by equation (5). The electric field E has y and z components and is written

$$E_y = \exp\left(\mathrm{i}\mathbf{k}\eta^{1/2}z\right) \sum_m s_m \exp\left(\mathrm{i}\mathbf{K}my\right) \tag{10 a}$$

$$E_z = \exp\left(\mathrm{i}\mathbf{k}\eta^{1/2}z\right) \sum_{m \neq 0} f_m \exp\left(\mathrm{i}\mathbf{K}my\right),\tag{10 b}$$

where s_m and f_m are constants. The curl Maxwell's equations are

$$\frac{\partial E_z}{\partial y} - \frac{\partial E_y}{\partial z} = -i\omega \mu_0 A$$

$$\frac{1}{\varepsilon} \frac{\partial A}{\partial z} = i\omega E_y$$

$$\frac{\partial A}{\partial y} = -i\omega \varepsilon E_z.$$
(11)

Identified in the plane wave basis, equations (11) become

$$m\mathbf{K}f_m - \mathbf{k}(\eta)^{1/2}s_m = -\omega\mu_0 A_m \tag{12 a}$$

$$\mathbf{k}(\eta)^{1/2} \sum_{1} a_{m-1} A_{1} = \omega s_{m} \tag{12 b}$$

$$m\mathbf{K}A_{m} = -\omega \sum_{1 \neq 0} \varepsilon_{m-1} f_{1}$$
 (12 c)

By substituting f_m from equation (12 a) into equation (12 c), and then using equation (12 b) to eliminate the y component of the electric field, we obtain the infinite set of linear equations

$$\forall i \neq 0 \quad (i\alpha^{2} - \varepsilon_{0}/i + \eta b_{ii})A_{i} + \sum_{1 \neq 0 \text{ and } i} \left(\eta b_{i1} - \frac{\varepsilon_{i-1}}{1}\right)A_{1} + \eta b_{i0}A_{0} = 0$$

$$(1 - \eta a_{0})A_{0} - \eta \sum_{1 \neq 0} a_{-1}A_{1} = 0,$$
(13)

where

$$b_{i1} = \sum_{p \neq 0} \frac{\varepsilon_{i-p} a_{p-1}}{p}.$$

Once again the effective relative permittivity η is seen as the value which obeys the dispersion relation

ae dispersion relation
$$-N\alpha^{2}-\epsilon_{0}/N+\eta b_{-N-N}\cdots \qquad \epsilon_{1-N}+\eta b_{-N-1} \quad \eta b_{-N0} -\epsilon_{-N-1}+\eta b_{-N1} \cdots -\epsilon_{-N-i}/i+\eta b_{-Ni}\cdots \\ \dots \qquad \dots \qquad \dots \qquad \dots \\ \dots \qquad \dots \qquad \dots \qquad \dots \\ \vdots \qquad \dots \qquad \dots \qquad \dots \\ -\alpha^{2}+\epsilon_{0}+\eta b_{-1-1} \quad \eta b_{-10} -\epsilon_{-2}+\eta b_{-11} \qquad -\epsilon_{-1}^{-1}-i/i+\eta b_{-1i}\cdots \\ -\eta a_{N} \qquad \qquad -\eta a_{1} \qquad 1-\eta a_{0} \qquad -\eta a_{1} \qquad \dots \\ \epsilon_{1-N}/N+\eta b_{1-N} \qquad \qquad \epsilon_{2}+\eta b_{1-1} \qquad \eta b_{10} \qquad \alpha^{2}-\epsilon_{0}+\eta b_{11} \qquad \dots \\ \epsilon_{i-N}/N+\eta b_{i-N} \qquad \dots \qquad \vdots \qquad \dots \\ \vdots \qquad \dots \qquad \dots \qquad \dots \qquad \dots$$

$$\epsilon_{i-N}/N+\eta b_{i-N} \qquad \dots \qquad \epsilon_{i+1}+\eta b_{i-1} \qquad \eta b_{i0} \qquad -\epsilon_{i-1}+\eta b_{i1} \qquad \dots \qquad \alpha^{2}-\epsilon_{0}/i+\eta b \qquad \dots \\ \dots \qquad \dots \qquad \dots \qquad \dots \qquad \dots \qquad \dots \qquad \dots$$

$$(144)$$

For a $(2N+1) \times (2N+1)$ determinant, equation (14) can be read as the nullity of a polynomial in α^2 of degree 2N. Substituting the asymptotic series of equation (4) into the determinant we easily derive that $1 - a_0 \eta_0 = 0$, so that the

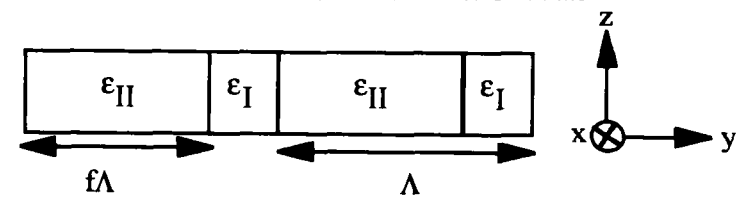


Figure 4. Lamellar structure composed of alternate layers of relarive permittivity ε_1 and ε_{II} . The fill factor f is a dimensionless coefficient equal to the ratio between the size of layer II and the period.

highest order in α^{4N} equals zero. Note that only the diagonal terms of the determinant contain α^2 terms. This can be exploited to derive η_2 by nullifying the coefficient of order (4N-2) of the polynomial. We obtain

$$\eta = \frac{1}{a_0} + \alpha^{-2} \frac{1}{a_0^3} \sum_{p \neq 0} \frac{a_{-p} b_{p0}}{p} + O(\alpha^{-4}). \tag{15}$$

To our knowledge, equation (15) has never been previously derived.

Let us now consider the particular example of figure 4 studied by Rytov [14]. A lamellar structure composed of two alternate layers of relative permittivities ε_I and ε_{II} is depicted. For this simple structure, the Fourier coefficient ε_n is

$$\varepsilon_n = \varepsilon_1 \delta_n + (\varepsilon_{11} - \varepsilon_1) \frac{\sin(\pi n f)}{\pi n},$$
(16)

where δ_n is non-zero and equals 1 if and only if n equals zero. f is the fill factor defined in figure 4. Using infinite summation of trigonometric Fourier series [24] and substituting the Fourier coefficients of equation (16) into equation (15), we obtain a simpler expression for η expressed as

$$\eta = \frac{1}{a_0} + \frac{\pi^2}{3} f^2 (1 - f)^2 \left(\frac{\varepsilon_{II} - \varepsilon_I}{\varepsilon_{II} \varepsilon_I} \right)^2 \frac{\varepsilon_0}{a_0^3} \alpha^{-2} + O(\alpha^{-4}). \tag{17}$$

By matching the boundary conditions inside the periodic structure, Rytov derives a transcendental equation (see equation (18) in [14]) which does not give an analytical solution for η . However using the Taylor series expansion for the tangents of the transcendental equation, equation (17) is derived. This coincidence is not fortuitous, since solving Maxwell's equations inside each layer and then matching the boundary conditions at the layer interfaces is equivalent to solving Maxwell's equations inside the whole periodic structure. As a consequence, equation (15) can be seen as a generalization of equation (17) for arbitrary profiles, including multi-layer lamellar (as in figure 2), sinusoidal or arbitrary continuously-varying-index periodic structures.

Finally, we note that equation (15) can also be derived by using a series expansion of A_i s in a similar manner as the authors of [16] did for TE polarization. This confirms to us the validity of such an expansion.

3.2. Simulation results

In order to test the validity of equation (15), we proceed as in section 2.3. A periodic structure with a continuous relative permittivity linearly varying from 1 to 9 over one period is chosen. As shown in figure 5, this structure is inserted between two infinite homogeneous regions of relative permittivities $\varepsilon_{\rm I}=1$ and

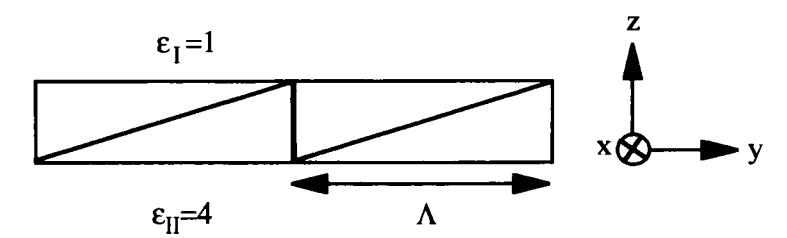


Figure 5. TM polarization case. A periodic structure with a continuously varying permittivity is inserted between two homogeneous regions of permittivities $\varepsilon_1 = 1$ and $\varepsilon_{11} = 4$. Along one period, the relative permittivity of the grating is linearly varying from 1 to 9. $h = 0.5\lambda$.

 $\varepsilon_{\rm II}=4$. Figure 5 defines a grating diffraction problem which is solved using RCWA, for a wave normally incident on the grating from the region of relative permittivity $\varepsilon_{\rm I}$. 501 orders were retained in the RCWA computation. It was largely sufficient since the same results were obtained with 401 retained orders. However, with 201 retained orders, like in the TE polarization case, convergence was not obtained, and highly inaccurate $n_{\rm RCWA}$ results were observed. The need for a very high number of retained orders to ensure proper convergence can be attributed to the fact that RCWA convergence-rates are much slower for TM than for TE polarization [25], and that the minimization problem of equation (9) is ill-conditioned. The comparison between the effective index prediction of equation (15) and RCWA simulation results is shown in figure 6. Again the solid line

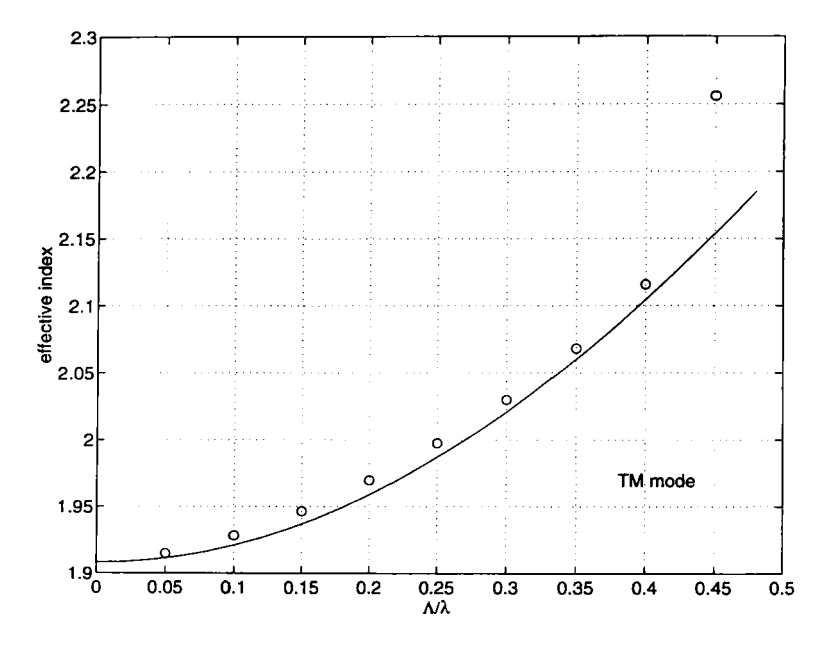


Figure 6. Simulation results for TM polarization. The solid curve represents the effective index of equation (15) when applied to the grating problem of figure 5. Circle-marks are the effective index n_{RCWA} obtained by minimizing the error function of equation (9). 501 orders were retained for the RCWA computation.

corresponds to the EMT prediction and the nine circle-marks result from RCWA computation. The horizontal axis covers the complete operating region of the grating as a zeroth-order filter for normal incidence. When determining the effective index n_{RCWA} , the maximum error e obtained with the first eight period-to-wavelength ratios $(\Lambda/\lambda = 0.05, 0.1, \dots, 0.4)$ is less than 0.06 and the maximum difference in reflected intensity $|r'(n_{\text{RCWA}})|^2 - |r|^2$ is less than 0.01.

The last circle-mark which does not match the EMT prediction deserves particular attention. Unlike the single point discrepancy of figure 3, the strong mismatch between EMT and RCWA for $\alpha = 0.45$ is not due to any problem caused by the ill-conditioning of the error-function minimization. For $\Lambda/\lambda=0.45$, the best effective index n_{RCWA} gives an error e = 0.43 and a difference in reflected intensity of 0.18. For Λ/λ larger than 0.33, we note that the effective index of the grating exceeds the cover and substrate indices, and so the grating of figure 5 becomes a waveguide grating. Because resonance effects in an evanescent wave cause a redistribution of the energy in the propagating waves, waveguide gratings can potentially generate sharp variations in the intensity of the reflected wave [26]. Even if EMT can be used to roughly estimate the wavelength at resonance, it cannot predict the energy redistribution around the resonance. For the grating problem of figure 5, a strong resonance effect was observed around $\alpha = 0.45$. The zeroth-order reflected intensity increases from 5% to 100% for Λ/λ varying from 0.450 to 0.457. This resonance effect explains the abnormally large error e and the discrepancy in figure 6 observed for Λ/λ equal to 0.45.

Because of the good matching between the solid line and the circle-marks in figure 6, we conclude that the simulation results validate the α^{-2} behaviour of the EMT solution. In general it was noted that the analogy between subwavelength structures and homogeneous media is less accurate in TM than in TE polarization, especially for large index-modulations.

4. EMT of symmetric two-dimensional periodic structures

The methodology used for deriving the zeroth- and second-order effective index of 2-D periodic structures is the same as the one used for 1-D periodic structures. However, the mathematical complexity is increased because of the double periodicity in the x and y directions. In section 4.1, we first derive the infinite set of linear equations that the wave propagating along the z axis must satisfy, from the Maxwell's equations. This linear system is similar to equations (6) and (13) previously derived for TE and TM polarization. In section 4.2, we solve the system of linear equations in the long wavelength limit, and derive the expression for the zeroth-order effective index. Section 4.3 provides simulation evidence showing that the zeroth-order effective index lies in between the upper and lower bounds derived by Coriell and Jackson [13]. In section 4.4 we derive the expression of the second-order effective index and, in section 4.5, we test our EMT result with RCWA.

In the following, we restrict the discussion to symmetric periodic structures with

$$\varepsilon_{m,n} = \varepsilon_{-m,n} = \varepsilon_{m,-n} = \varepsilon_{-m,-n}. \tag{18}$$

Note that it does not imply the equality of the periods along the x and y directions, but simply that a centre of symmetry exists.

4.1. Derivation of the infinite set of linear equations

In the appendix, using the Floquet theorem, we derive the following set of second-order differential equations

$$S''_{y00} + \mathbf{k}^{2} \sum_{p,q} \varepsilon_{-p,-q} S_{ypq}$$

$$= 0$$

$$S''_{x00} + \mathbf{k}^{2} \sum_{p,q} \varepsilon_{-p,-q} S_{xpq}$$

$$= 0$$
(19 a)

$$m\rho S_{ymn}'' - nS_{xmn}'' + \mathbf{K}^2(n^2 + m^2\rho^2)(nS_{xmn} - m\rho S_{ymn}) + \mathbf{k}^2\sum_{p,q}\varepsilon_{m-p,\,n-q}(m\rho S_{ypq} - nS_{xpq})$$

$$=0 (19c)$$

$$\mathsf{K}^2 \sum_{p,\,q} \varepsilon_{m-p,\,n-q} (m \rho S_{xpq} + n S_{ypq})$$

$$= \sum_{(p,q)\neq(0,0)} \frac{\varepsilon_{m-p,n-q}}{p^2 \rho^2 + q^2} \left(q S_{ypq}'' + p \rho S_{xpq}'' + \mathbf{k}^2 \sum_{r,t} \varepsilon_{p-r,q-t} (p \rho S_{xrt} + q S_{yrt}) \right). \quad (19 \ d)$$

The last two equations (19 c) and (19 d) hold for any m and n, $(m, n) \neq (0, 0)$. S_{xmn} and S_{ymn} are the (m, n)th space-harmonic amplitudes of the electric field's x and y components. They only depend on z. S''_{xmn} and S''_{ymn} are the second derivatives $\partial^2 S_{xmn}/\partial z^2$ and $\partial^2 S_{ymn}/\partial z^2$, respectively. Equations (19) provide a complete set of second-order differential equations (Helmholtz equations) for the x and y components of the electric fields inside 2-D periodic structures. They are formally equivalent to equations (22) of [25].

We look for a wave with the z-dependence of equation (3), which satisfies equations (19). The x and y components of the wave electric field are

$$E_x = \exp(i\mathbf{k}\eta^{1/2}z) \sum_{(m, n) \neq (0, 0)} s_{xmn} \exp[i\mathbf{K}(m\rho x + ny)]$$
 (20 a)

$$E_{y} = \exp\left(\mathrm{i}\mathbf{k}\eta^{1/2}z\right) \sum_{m,n} s_{ymn} \exp\left[\mathrm{i}\mathbf{K}(m\rho x + ny)\right],\tag{20 b}$$

where s_{xmn} and s_{ymn} are constants, and only E_y has a dc component. On spatial averaging along the x and y directions of the periodic structure, E_x equals zero and E_y equals s_{y00} , since only E_x has a non-null dc component. Note that when looking for a wave polarized in the x direction, equations (20) hold except that, in this case, only E_x has a dc component (i.e. $s_{y00} = 0$ and $s_{x00} \neq 0$). In the following, the EMT for the x polarization will not be derived. Its derivation is basically the same as the y polarization case, and therefore only its result will be given. Because of the symmetry hypothesis of equation (18), it is readily apparent that for any (m, n),

$$s_{xmn} = -s_{x-mn} = -s_{xm-n} = s_{x-m-n}$$
 and $s_{ymn} = s_{y-mn} = s_{ym-n} = s_{y-m-n}$. (21)

Equation (21) implies that, for any p, s_{xp0} and s_{x0p} are equal to zero. Substituting S_{lmn} and S''_{lmn} with s_{lmn} and $-\mathbf{k}^2\eta s_{lmn}$ (l holds for x and y) into equations (19), we

obtain the following set of linear equations

$$\eta s_{y00} = \sum_{p, q} \varepsilon_{pq} s_{ypq}, \qquad (22 a)$$

and $\forall m \ge 0, \forall n \ge 0, (m, n) \ne (0, 0),$

$$\alpha^2(n^2+m^2\rho^2)(ns_{xmn}-m\rho s_{ymn})$$

$$= m\rho\eta s_{ymn} - n\eta s_{xmn} - \sum_{p,q} \varepsilon_{m-p,n-q} (m\rho s_{ypq} - ns_{xpq}) = 0$$
 (22 b)

$$\alpha^2 \sum_{p,q} \varepsilon_{m-p,n-q} (m \rho s_{xpq} + n s_{ypq})$$

$$=\sum_{(p,q)\neq(0,0)}\frac{\varepsilon_{m-p,n-q}}{p^2\rho^2+q^2}\left(-q\eta s_{ypq}-p\rho\eta s_{xpq}+\sum_{r,t}\varepsilon_{p-r,q-t}(p\rho s_{xpq}+qs_{ypq})\right). \quad (22\ c)$$

Note that equation (19 b) becomes trivial. Of course equations (22 b) and (22 c) hold for any $(m, n) \neq (0, 0)$, but because of the symmetry, we need only to consider these equations for positive m and n values. Equations (22) correspond to equations (6) and (13) previously derived for 1-D periodic structures.

4.2. Zeroth-order effective index

As equations (22) are a complete set of equations, in principle the dispersion relation can be written by nullifying the determinant of the set of equations. But for this 2-D problem, the determinant cannot be simply expressed. In order to derive the EMT, it is preferable to assume that s_{ymn} and s_{xym} can be expanded in a power series of Λ/λ . The validity of this assumption was discussed in section 2.2. We note the power series expansion

$$s_{vmn} = s_{vmn}^{(0)} + \alpha^{-2} s_{vmn}^{(2)} + \cdots$$
 (23 a)

$$s_{xmn} = s_{xmn}^{(0)} + \alpha^{-2} s_{xmn}^{(2)} + \cdots,$$
 (23 b)

where odd-order terms are omitted since equations (22) only depend on α^2 . By retaining terms in α^0 in equation (22 a) and in α^2 in equations (22 b) and (22 c), we obtain

$$(\eta_0 - \varepsilon_{0,0}) s_{y00}^{(0)} = \sum_{\substack{(p,q) \neq (0,0)}} \varepsilon_{p,q} s_{ypq}^{(0)}, \tag{24 a}$$

and $\forall m \ge 0, \forall n \ge 0, (m, n) \ne (0, 0),$

$$\sum_{p,q} \varepsilon_{m-p,n-q} (m\rho s_{xpq}^{(0)} + ns_{ypq}^{(0)}) = 0$$
 (24b)

$$ns_{xmn}^{(0)} = m\rho s_{ymn}^{(0)}. (24c)$$

Using equation (24 c) to express $s_{xmn}^{(0)}$ as a function of $s_{ypq}^{(0)}$, and substituting into equation (24 b), we obtain for positive n and m with $(m, n) \neq (0, 0)$

$$\sum_{p,q\neq 0} \varepsilon_{m-p,n-q} \left(n + \frac{mp\rho^2}{q} \right) s_{ypq}^{(0)} = -n\varepsilon_{m,n} s_{y00}^{(0)}, \tag{25}$$

From equation (24 c), $s_{ym0}^{(0)}$ equals zero for non-zero m. According to equation (21), for n = 0, equation (25) is trivial. If the Fourier series is truncated to $\pm M_{\rm EMT}$

orders both in the x and y directions, equation (25) can be read as a system of $M_{\rm EMT}(M_{\rm EMT}+1)$ equations $(\forall m \ge 0, \forall n > 0)$, which can be set in the compact form

 $\mathbf{A}\mathbf{s}_{y}^{(0)} = -s_{y00}^{(0)}\mathbf{b} \tag{26}$

where **A** is a $M_{\rm EMT}(M_{\rm EMT}+1)$ by $M_{\rm EMT}(M_{\rm EMT}+1)$ matrix, $\mathbf{s}_y^{(0)}$ is a $M_{\rm EMT}(M_{\rm EMT}+1)$ vector composed of $s_{ypq}^{(0)}$ elements, and **b** is a $M_{\rm EMT}(M_{\rm EMT}+1)$ vector with $n\varepsilon_{m,n}$ elements. We suppose that **A** can be inverted (we have no demonstration of that point). Denoting by **a** the inverse matrix of **A**, $s_{ypq}^{(0)}$ can be expressed as a function of $s_{y00}^{(0)}$, and we have

$$\forall p \ge 0, \ \forall q > 0, \ s_{ypq}^{(0)} = -s_{y00}^{(0)} \sum_{m \ge 0, n > 0} a_{m,n}^{p,q} \varepsilon_{m,n} n,$$
 (27)

where $a_{m,n}^{p,q}$ are the coefficients of matrix **a**. These coefficients only depend on the periodic structure, i.e. on $\varepsilon_{m,n}$ and ρ . Substituting $s_{ypq}^{(0)}$ given by equation (27) into equation (22 a), and looking for a non-zero solution in $s_{y00}^{(0)}$, we obtain the zeroth-order effective permittivity

$$\eta_0 = \varepsilon_{0,0} - \sum_{p,q \neq 0} \sum_{m \geq 0, n > 0} \varepsilon_{m,n} a_{m,n}^{p,q} \varepsilon_{p,q} n. \tag{28}$$

When considering a wave polarized in the x direction, equation (25) has to be replaced by

$$\sum_{\mathbf{p}\neq 0,\,\mathbf{q}} \varepsilon_{m-p,\,n-q} \left(m + \frac{nq}{p\rho^2} \right) s_{xpq}^{(0)} = -m \varepsilon_{m,\,n} s_{x00}^{(0)}, \tag{29}$$

which holds for $n \ge 0$ and m > 0. Equation (29) defines a new matrix $\hat{\mathbf{A}}$ and a new vector $\hat{\mathbf{b}}$, where carats are used for differentiating the x and y polarization case. So for the x polarization, the zeroth-order effective permittivity $\hat{\eta}$ is

$$\hat{\eta} = \varepsilon_{0,0} - \sum_{p \neq 0, q} \sum_{m > 0, n \geq 0} \varepsilon_{m,n} \hat{a}_{m,n}^{p,q} \varepsilon_{p,q} m, \tag{30}$$

where $\hat{a}_{m,n}^{p,q}$ are the coefficients of the inverse matrix of $\hat{\mathbf{A}}$. In general, because $(\hat{\mathbf{A}}, \hat{\mathbf{b}})$ and (\mathbf{A}, \mathbf{b}) are different, the two normal effective indices are also different, and the periodic structure exhibits biaxial properties in the long wavelength limit. Now when we assume that $\varepsilon_{m,n}$ and $\varepsilon_{n,m}$ are equal for any (m,n) and that the periods in the x and y direction are the same $(\rho = 1)$, it is easily shown that $(\hat{\mathbf{A}}, \hat{\mathbf{b}})$ and (\mathbf{A}, \mathbf{b}) are equal, and so the periodic structure exhibits uniaxial properties.

4.3. Zeroth-order effective index: simulation results

Coriell and Jackson [13] derived upper and lower bound expressions for the zeroth-order EMT of several simple symmetric periodic structures composed of two-phase materials. The two structures they considered are depicted in figure 7. They are both symmetric with $\varepsilon_{m,n} = \varepsilon_{n,m}$ and $\rho = 1$, and are composed of two homogeneous media indexed by 1 and 2. In our simulation, media 1 and 2 have optical permittivities equal to 1 and 16, respectively. The periodic structure of figure 7(a) is composed of parallelepipeds of high index inserted in a medium of low index. Similarly, the periodic structure of figure 7(b) is composed of cylinders of low index inserted in a medium of high index. We define the fill factor of the two structures as the ratio between the width (resp. the diameter) of the parallelepiped (resp. cylinder) and the period Λ . For these two periodic structures,

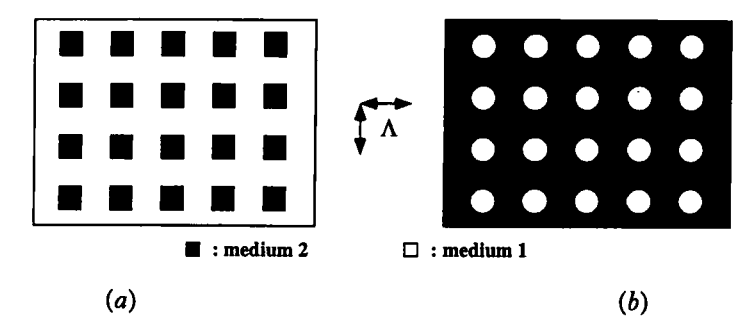


Figure 7. (a) Periodic structure composed of parallelepipeds of high index inserted in a medium of low index. (b) Periodic structure composed of cylinders of low index inserted in a medium of high index.

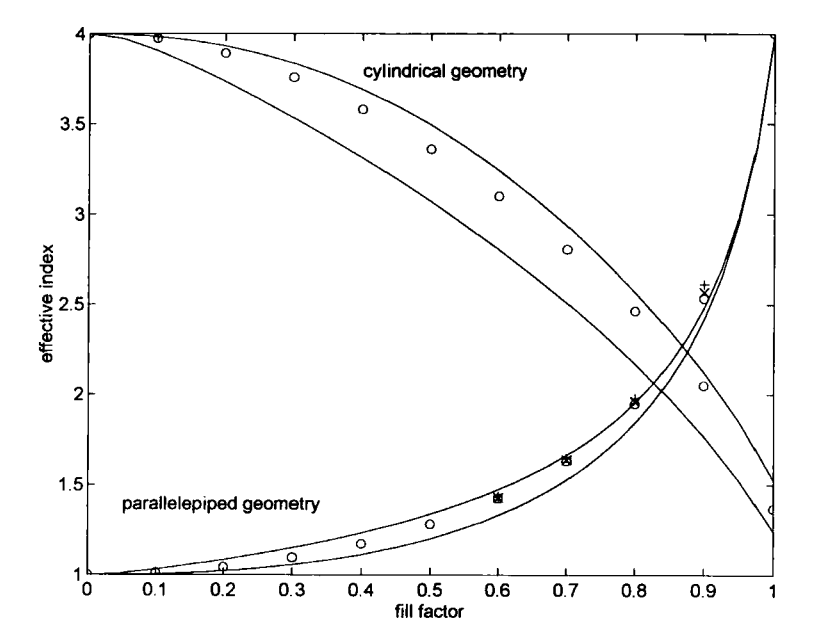


Figure 8. Zeroth-order effective index of the 2-D periodic structures. The solid curves are the upper and lower bounds derived in [13] for the zeroth-order effective index and for the periodic structure of figure 7. Plus-marks, cross-marks and circle-marks are, respectively, the effective indices of equation (28) for truncation ranks $M_{\rm EMT}$ equal to 8, 20 and 40.

the upper and lower bounds are given by equations (6 a), (6 b), (7 a) and (7 b) of [13]. They are plotted in figure 8 as a function of the fill factor. These are the solid curves in figure 8. As we could not find a general expression for the inverse matrix a, only numerical computations allow us to derive the values of η_0 given by equation (28). The computation basically requires the inversion of the infinite matrix A, which for numerical purposes is truncated. We denote by $M_{\rm EMT}$ the truncation rank. The size of the truncated matrix is $M_{\rm EMT}(M_{\rm EMT}+1)\times M_{\rm EMT}(M_{\rm EMT}+1)$. Because of the symmetry (equation (21)), a truncation rank $M_{\rm EMT}$ corresponds to $\pm M_{\rm EMT}$ orders in each direction, i.e. a total of $N=(2M_{\rm EMT}+1)^2$ orders. In figure 8, circle-, cross-, and plus-marks are the effective indices obtained for different

truncation ranks of matrix A. Circle-marks were derived with $M_{\rm EMT}=40~(N=6561)$, cross-marks with $M_{\rm EMT}=20~(N=1681)$, and plus-marks with $M_{\rm EMT}=7~(N=225)$. Basically, the EMT prediction of equation (28) lies in between the upper and lower bounds. For the parallelepiped case and for fill factors about 0.8 and 0.9, it is noticeable that the truncated expansion is slowly converging. For a fill factor equal to 0.9, even with $M_{\rm EMT}=40$, η_0 remains just above the upper bound.

4.4. Second-order effective index

We now proceed to the derivation of the second-order EMT. Taking α^{-2} terms in equation (22 a) and α^{0} terms in equations (22 b) and (22 c) and simplifying using equations (24 b) and (24 c), we obtain

$$\eta_0 s_{y00}^{(2)} + \eta_2 s_{y00}^{(0)} = \sum_{p,q} \varepsilon_{p,q} s_{ypq}^{(2)},$$
(31 a)

and $\forall m \ge 0, \forall n \ge 0, (m, n) \ne (0, 0),$

$$\sum_{p,q} \varepsilon_{m-p,n-q} (m\rho s_{xpq}^{(2)} + ns_{ypq}^{(2)}) = -\eta_0 \sum_{(p,q) \neq (0,0)} \frac{\varepsilon_{m-p,n-q}}{p^2 \rho^2 + q^2} (p\rho s_{xpq}^{(0)} + qs_{ypq}^{(0)}) \quad (31 b)$$

$$(n^2 + m^2 \rho^2)(ns_{xmn}^{(2)} - m\rho s_{ymn}^{(2)}) = -\sum_{p,q} \varepsilon_{m-p,n-q}(m\rho s_{ypq}^{(0)} - ns_{xpq}^{(0)}). \tag{31 c}$$

For n = 0, equation (31 c) reduces to

$$\forall m > 0, \ s_{ym0}^{(2)} = \frac{1}{m^2 \rho^2} \sum_{p,q \neq 0} \varepsilon_{m-p,q} s_{ypq}^{(0)} + \varepsilon_{m,0} s_{y00}^{(0)}. \tag{32}$$

As $s_{xpq}^{(0)}$ can be expressed as a function of $s_{ypq}^{(0)}$, equation (31 c) allows us to express $s_{xmn}^{(2)}$ as a function of $s_{ypq}^{(0)}$ and $s_{ymn}^{(2)}$. Substituting into equation (31 b) $s_{xmn}^{(2)}$ by its expression as function of $s_{ypq}^{(0)}$ and $s_{ymn}^{(2)}$, we obtain

$$\forall m \ge 0, \forall n > 0, \sum_{p,q \ne 0} \varepsilon_{m-p,n-q} \left(n + \frac{m\rho^2 p}{q} \right) s_{ypq}^{(2)} = c_{mn} s_{y00}^{(0)} - \varepsilon_{mn} n s_{y00}^{(2)}, \quad (33)$$

where

$$c_{mn}s_{y00}^{(0)} = \sum_{p,q\neq 0} \varepsilon_{m-p,n-q} \left(\frac{\varepsilon_{p,q} m \rho^2 p}{q(\rho^2 p^2 + q^2)} s_{y00}^{(0)} - \frac{\eta_0}{q} s_{ypq}^{(0)} + m \rho^2 \sum_{r,t\neq 0} \frac{\varepsilon_{p-r,q-t}}{\rho^2 p^2 + q^2} \left(\frac{p}{q} - \frac{r}{t} \right) s_{yrt}^{(0)} \right) - \sum_{p\neq 0} \varepsilon_{m-p,n} n s_{yp0}^{(2)}.$$
(34)

The right term of equation (34) is only a function of $s_{y00}^{(0)}$ since $s_{yp0}^{(2)}$ and $s_{ypq}^{(0)}$ are only functions of $s_{y00}^{(0)}$ (see equations (27) and (32)). Consequently vector \mathbf{c} , whose coefficients are c_{mn} , is only dependent on the periodic structure, i.e. on ε_{mn} and ρ . Equation (33) can be written in the compact form

$$\mathbf{A}\mathbf{s}_{y}^{(2)} = s_{y00}^{(0)}\mathbf{c} - s_{y00}^{(2)}\mathbf{b}, \tag{35}$$

where matrix A and vector b are the same as in equation (26). So the solution of equation (35) can be written

$$\forall p \ge 0, \forall q > 0, s_{ypq}^{(2)} = \sum_{m \ge 0, n > 0} a_{m,n}^{p, q} (c_{mn} s_{y00}^{(0)} - \varepsilon_{m,n} n s_{y00}^{(2)}).$$
 (36)

By substituting $s_{ypq}^{(2)}$ from equations (36) and (32) into equation (31 a), the $s_{y00}^{(2)}$ term cancels. By looking for a non-zero solution in $s_{ypq}^{(0)}$, we obtain the second-order effective relative permittivity

$$\eta_{2} = \sum_{p,q \neq 0} \sum_{m \geqslant 0, n > 0} \varepsilon_{p,q} a_{m,n}^{p,q} c_{mn} + \sum_{p \neq 0} \frac{\varepsilon_{p,0}}{p^{2} \rho^{2}} \left(\varepsilon_{p,0} - \sum_{\substack{(r,t) \neq (0,0) \\ v \geqslant 0, v > 0}} \varepsilon_{p-r,t} a_{r,t}^{u,v} \varepsilon_{r,t} t \right). \tag{37}$$

A similar expression with $\hat{a}_{m,n}^{p,q}$ coefficients holds for the x polarization case.

4.5. Second-order effective index: simulation results

In order to verify the validity of equation (37), we proceed as in sections 2.3 and 3.2, and we insert a one-wavelength thick layer of the periodic structure, as shown in figure 7(a), into two semi-infinite homogeneous media of relative permittivities 1 and 16. For Λ/λ smaller than 0.25, this defines a zeroth-order grating problem that is solved by rigorous computation. The fill factor was chosen equal to 0.6. For 2-D periodic structures, the implementation of coupled-wave methods is memory consuming, With our IBM/RISC6000 workstation, only 289 retained orders can be implemented in the RCWA computation. As was noted in section 2.3, the minimization of the error function of equation (9) is not wellconditioned. Moreover in section 4.3, the truncated expansion used in our EMT derivation which, like coupled-wave methods, depends on the Fourier expansion of the grating relative permittivity, was shown to be slowly converging especially for a duty cycle equal to 0.9. Being aware of the difficulty of obtaining very accurate rigorous computations, and of their impact when carefully comparing them with EMT predictions, we asked our colleagues at the Helsinki University of Technology to run their highly efficient code implementation. We are grateful to Eero Noponen, who computed for us the transmitted and reflected amplitudes, using his eigenmode method for three-dimensional profiles [27]. The transmitted and reflected amplitudes, t and r, he found with 625 retained orders, are shown in the second and fourth columns of table 1. The corresponding period-to-wavelength ratios are given in the first column. In table 2, the convergence of the coupled-wave used in the simulation is illustrated. The reflected and transmitted amplitudes are given for different numbers N of retained orders varying from 289 to 625. These results

Table 1. Reflection and transmission complex coefficients of the period structure of figure 7(a) when inserted between two semi-infinite media of relative permittivities 1 and 16. The r and t coefficients are the reflection and transmission complex coefficients obtained when retaining 625 orders in RCWA, and the r" and t" coefficients are those predicted by the second-order EMT (index given by the two first non-zero terms of equation (4)). The corresponding period-to-wavelength ratios are shown in column 1.

Λ/λ	r	r"	t	t"
0.02	-0.517 + 0.265i	-0.4521 + 0.3394i	-0.390 + 0.116i	-0.378 + 0.165i
0.05	-0.531 + 0.242i	-0.4808 + 0.3094i	-0.395 + 0.094i	-0.383 + 0.147i
0.075	-0.551 + 0.202i	-0.5175 + 0.2621i	-0.400 + 0.064i	-0.388 + 0.122i
0.1	-0.570 + 0.137i	-0.5570 + 0.1925i	-0.404 + 0.023i	-0.394 + 0.088i
0.15	-0.548 - 0.088i	-0.5999 - 0.0102i	-0.401 - 0.111i	-0.400 - 0.005i
0.12	-0.158 - 0.321i	-0.5158 - 0.2528i	-0.270 - 0.381i	-0.388 - 0.129i
0.24	0.069 + 0.295i	-0.3084 - 0.3883i	0.263 + 0.398i	-0.347 - 0.261i

Table 2. Convergence of the coupled-wave method. The first column shows the number N of retained orders in the computation. r and t are, respectively, the reflection and transmission complex coefficients. $\Lambda/\lambda = 0.1$.

N	r	t	
289	-0.5819 + 0.0849i	-0.4044 + 0.0001i	
361	-0.5813 + 0.0870i	-0.4045 + 0.0006i	
441	-0.5746 + 0.1195i	-0.4045 + 0.0156i	
529	-0.5724 + 0.1276i	-0.4046 + 0.0190i	
625	-0.5698 + 0.1366i	-0.4045 + 0.0230i	

are obtained for $\alpha = 0.1$. As can be seen, even with 625 orders, the convergence of the rigorous computation is not perfectly guaranteed. Although the real part of t is constant for the considered interval (variation less than 10^{-4}), we note that r and the imaginary part of t are gradually increasing. This effect is weak, since from N = 289 to N = 625, the variations observed on the real and imaginary parts of r and t are smaller than 0.05. Thus, for the following comparison, we will consider the reflection and transmission coefficients computed with 625 retained orders as enough accurate to allow a qualitative comparison with our EMT results.

For the numerical computation of the EMT, we proceed as follows. Once matrix A is inverted and $a_{m,n}^{p,q}$ are known, $s_{ypq}^{(0)}$ and $s_{ypq}^{(2)}$ are computed with equations (27), (32) and (36). Then η_0 and η_2 are numerically derived by using equations (28) and (37), where $s_{y00}^{(0)}$ and $s_{y00}^{(2)}$, are, respectively, set to 1 and 0. When inverting matrix A, the truncation rank $M_{\rm EMT}$ was chosen equal to 40. A truncation rank of 40 corresponds to 6561 retained orders with the coupled-wave method, and thus can be considered to be large enough to be accurate. The reflected and transmitted amplitudes found by replacing the grating by the homogeneous layer with the effective index predicted by the EMT are noted r'' and t'', respectively. They are shown in the third and fifth columns of table 1. This allows a direct visual comparison with the r and t coefficients computed by the rigorous method. According to table 1, two operating regions can be distinguished for the comparison. For Λ/λ larger than 0.15, there is no match between rigorous computation and EMT prediction. For Λ/λ smaller than 0.15, the real parts of the transmitted amplitude t'' predicted by EMT never differ by more than 0.01 from the rigourous computation results, and the difference between the imaginary parts of the transmitted amplitudes (t and t''), and between the real and imaginary parts of the reflected amplitudes (r and r") is never larger than 0.07. This corresponds to a difference between the reflected or transmitted intensities which is never larger than 0.02. Thus, we first conclude that, for Λ/λ smaller than 0.15, a good qualitative agreement between EMT and rigorous computation is obtained. In table 3, a comparison between the effective index n_{RCWA} derived from rigorous computations and the second-order EMT prediction $\eta^{1/2}$ is shown. For Λ/λ smaller than 0.15, a small difference between n_{RCWA} and $\eta^{1/2}$ exists. The difference is smaller than 0.02. For Λ/λ larger than 0.15, the difference is significantly larger and reaches 0.2 for $\Lambda/\lambda = 0.15$.

The poor agreement between EMT and rigorous computation for large

Table 3. First column, period-to-wavelength ratios. Second and third column, errors and effective indices found by minimizing equation (9). Last column, EMT effective indices given by the two first non-zero terms of equation (4).

Λ/λ	e	n _{RCWA}	$\eta^{1/2}$
0.02	0.008	1.443	1.424
0.05	0.020	1.448	1.432
0.075	0.031	1.457	1.443
0.1	0.048	1.471	1.459
0.15	0.035	1.527	1.502
0.2	0.093	1.665	1.561
0.24	0.168	1.808	1.618

period-to-wavelength ratio raises the following question. Has this bad agreement to be attributed to the EMT itself, or to the fact that for large period-to-wavelength ratios, a strict analogy between 2-D periodic structures and homogeneous media does not exist? To answer this question, we solve the minimization problem defined by equation (9). For $\Lambda/\lambda = 0.2$ and 0.24, the two effective indices found are $n_{\text{RCWA}} = 1.665$ and $n_{\text{RCWA}} = 1.808$ (see table 3). The corresponding errors e are large, and are, respectively, equal to 0.093 and to 0.168 (see table 3). For comparison, for the 1-D grating of section 2.3 which has a comparable index modulation, the maximum error found was 0.06. We thus conclude that the analogy does not hold for large period-to-wavelength ratios. This poor analogy observed for 2-D structures (in comparison with 1-D structures) can be justified by looking at the long-wavelength-limit behaviour difference of 1-D and 2-D periodic structures. By expanding the diffracted wave amplitudes A_i in a power series of α^{-1} , for TE and TM polarization of 1-D structures, it is easily shown that [16]

$$\forall i \neq 0, A_i = O(\alpha^{-2})$$
 and $A_0 = O(\alpha^0)$. (38)

Consequently, in the long wavelength-limit, waves which propagate in 1-D periodic structures are simply plane waves $A_0 \exp(i\eta_0^{1/2}\mathbf{k}z)$, with $\eta_0 = \varepsilon_0$ for TE or $\eta_0 = 1/a_0$ for TM. For 2-D periodic structures, the wave is no longer a plane wave, but a superposition of plane waves, since neither $s_{xmn}^{(0)}$ nor $s_{ymn}^{(0)}$ are zero for $(m, n) \neq (0, 0)$. So 2-D period structures are not strictly equivalent to homogeneous media even for infinitely small periods. It is thus reasonable to see that, for large period-to-wavelength ratios near the cutoff value, the analogy between 2-D periodic structures and homogeneous media is even less accurate or legitimate.

Conclusion

In this paper, the EMT of 1-D and 2-D periodic structures was studied for waves propagating normally to the structure. For 1-D periodic structures, a closed-form of the zeroth- and second-order effective indices was derived for TE and TM polarization (see equations (8) and (15)). These formulas can be applied to any arbitrary periodic structures, symmetric or not, with continuously-varying-

index profiles or step-index profiles. The validity of equations (8) and (15) was tested by RCWA, and a very good agreement between the EMT results and RCWA simulation results was obtained, even for large periods that almost reach the cutoff period above which the gratings stop to behave as zeroth-order filters. For 2-D periodic structures, formulas for the zeroth- and second-order effective indices of symmetric periodic structures were derived (see equations (28) and (37)). These formulas can be applied to any arbitrary periodic structures which have a centre of symmetry. The numerical evaluation of equations (28) and (37) requires the inversion of the same infinite matrix. In practice, the matrix is truncated and is inverted numerically with standard library programs. We have shown that the zeroth-order EMT (equation (28)) lies in between the lower and upper bounds derived in [13]. When validating the second-order EMT by rigorous computation, a good qualitative agreement between the EMT and simulation results was obtained. However, it was found that the analogy between subwavelength periodic structures and homogeneous media is less accurate for 2-D than for 1-D structures. For periods larger than half the cutoff period, the periodic structure of our example stops behaving as a homogeneous medium. In the paper, although all simulation results are provided for real index profiles, the EMT results can also be used for absorptive materials.

Acknowledgments

When this work was completed, Ph. Lalanne was a visiting scientist at the Institute of Optics at the University of Rochester. He is pleased to acknowledge the Direction Générale de l'Armement for financial support under contract DRET-DGA #94-1123. The authors are grateful to Professor G. M. Morris for fruitful discussions, and to Eero Noponen for his kind help in the simulation of section 4.5.

Appendix

In this appendix, we derive equations (19). For the sake of generality, the $\exp(i\eta^{1/2}\mathbf{k}z)$ dependence of equation (3) is first not assumed, and we derive a set of second-order differential equations using the Floquet theorem. This formulation is similar to that provided by Peng and Morris in [28], in which electromagnetic scattering of 2-D gratings was analysed by using RCWA with second-order differential equations. For ease of reference, we shall follow the notation used in this work.

As the periods in the x and y directions are respectively noted by Λ/ρ and Λ , the electric and magnetic fields E_x and H_x are expressed as (Floquet theorem)

$$E_{x} = \sum_{m,n} S_{xmn} \exp\left[i\mathbf{K}(m\rho x + ny)\right]$$

$$H_{x} = \left(\frac{\varepsilon_{0}}{\mu_{0}}\right)^{1/2} \sum_{m,n} U_{xmn} \exp\left[i\mathbf{K}(m\rho x + ny)\right],$$
(A1)

where S_{xmn} and U_{xmn} depend on variable z. Similar expressions hold for the y and z polarization of the field. We denote by S_{ymn} , S_{zmn} , U_{ymn} , and U_{zmn} their dependence with z. The curl Maxwell's equations identified in the quasi-plane

wave basis are

$$in\mathbf{K}S_{xmn} - S'_{ymn} + i\mathbf{k}U_{ymn} = 0 (A2 a)$$

$$-\mathrm{i}m\rho \mathbf{K} S_{nmn} + S'_{nmn} + \mathrm{i}\mathbf{k} U_{nmn} = 0 \tag{A2b}$$

$$m\rho \mathbf{K} S_{vmn} - n \mathbf{K} S_{xmn} + \mathbf{k} U_{zmn} = 0$$
 (A2c)

$$in\mathbf{K} U_{xmn} - U'_{ymn} - i\mathbf{k} \sum_{p,q} \varepsilon_{m-p,n-q} S_{xpq} = 0$$
 (A 2d)

$$-\mathrm{i}m\rho \mathbf{K} U_{zmn} + U'_{xmn} - \mathrm{i}\mathbf{k} \sum_{p,q} \varepsilon_{m-p,n-q} S_{ypq} = 0$$
 (A2 e)

$$m\rho \mathbf{K} U_{ymn} - n\mathbf{K} U_{xmn} - \mathbf{k} \sum_{p,q} \varepsilon_{m-p,n-q} S_{xpq} = 0,$$
 (A2 f)

where prime denotes the derivative relatively to the z-variable. We now proceed with the elimination of U_x , U_y , U_z and S_z in between the six previous equations. As can be seen from our previous work on TE and TM polarization of 1-D gratings, we try to derive second-order differential equations containing a minimum number of terms depending on α , or similarly on **K**. Setting m = n = 0 in equations (A2), we first obtain equations (19 a) and (19 b) which do not depend on parameter **K**.

From equations (A2d) and (A2e), we obtain

$$(n^2 + m^2 \rho^2) \mathbf{K} U_{xmn} + \mathrm{i} n U_{ymn}^{'-} + \mathrm{i} m \rho U_{xmn}^{'} + \mathbf{k} \sum_{p,q} \varepsilon_{m-p,\,n-q} (m \rho S_{ypq} - n S_{xpq}) = 0$$

(A3a)

$$nU'_{xmn} - m\rho U'_{ymn} - \mathrm{i}\mathbf{k} \sum_{p,q} \varepsilon_{m-p,n-q} (m\rho S_{xpq} + nS_{ypq}) = 0.$$
(A3b)

From equation (A2 c), U_{zmn} can be expressed as a function of S_{ymn} and S_{xmn} . From $\nabla H = 0$ that can be derived from equations (A2 a)-(A2 c), and from equation (A3 a), equation (19 c) is derived for any $(m, n) \neq (0, 0)$. From equation (A3 b) and (A2 f), we obtain

$$\sum_{p,q} \varepsilon_{m-p,n-q} S'_{zpq} = -i \mathbf{K} \sum_{p,q} \varepsilon_{m-p,n-q} (m \rho S_{xpq} + n S_{ypq}), \tag{A4}$$

which is simply $\nabla(\varepsilon \mathbf{E}) = 0$. From equations (A2 a) and (A2 b), we have

$$i\mathbf{K}S'_{zmn} = \frac{1}{n^2 + m^2\rho^2} (nS''_{ymn} + m\rho S''_{xmn} - i\mathbf{k}(nU'_{xmn} - m\rho U'_{ymn})).$$
 (A5)

Substituting $nU'_{xmn} - m\rho U'_{ymn}$ from equation (A3b) and (A5), S_{xmn} is seen only as a function of S_y and S_x . Substituting S_{xmn} into equation (A4), equation (19d) is derived for any $(m, n) \neq (0, 0)$.

References

- [1] Wilson, S. J., and Hutley, M. C., 1982, Optica Acta, 29, 993.
- [2] ENGER, R. C., and CASE, S. K., 1983, Appl. Optics, 22, 3220.
- [3] GAYLORD, T. K., BAIRD, W. E., and MOHARAM, M. G., 1986, Appl. Optics, 25, 4562.
- [4] Ono, Y., Kimura, Y., Otha, Y., and Nishida, N., 1987, Appl. Optics, 26, 1142.

- [5] MOTAMEDI, M. E., SOUTHWELL, W. H., and GUNNING, W. J., 1992, Appl. Optics, 31, 4371.
- [6] RAGUIN, D. H., and MORRIS, G. M., 1993, Appl. Optics, 32, 1154.
- [7] CESCATO, L. H., GLUCH, E., and STREIBL, N., 1990, Appl. Optics, 29, 3286.
- [8] Flanders, D. C., 1983, Appl. Phys. Lett., 42, 492.
- [9] YEH, P., 1978, Optics Commun., 26, 289.
- [10] STORK, W., STREIBL, N., HAIDNER, H., and KIPFER, P., 1991, Optics Lett., 16, 1921.
- [11] FARN, W. M., 1992, Appl. Optics, 31, 4453.
- [12] CHEN, F. T., and CRAIGHEAD, H. G., 1995, Optics Lett., 20, 121.
- [13] Coriell, S. R., and Jackson, J. L., 1968, J. Appl. Phys., 39, 4733.
- [14] RYTOV, S. M., 1956, Sov. Phys. JETP, 2, 466.
- [15] McPhedran, R. C., Botten, L. C., Craig, M. S., Nevière, N., and Maystre, D., 1982, Optica Acta, 29, 289.
- [16] Bell, J. M., Derrick, G. H., and McPhedran, R. C., 1982, Optica Acta, 29, 1475.
- [17] BOUCHITTE, G., and PETIT, R., 1985, Electromagnetics, 5, 17.
- [18] HAGGANS, C. W., LI, L., and KOSTUK, R. K., 1993, J. opt. Soc. Am. A, 10, 2217.
- [19] CAMPBELL, G., and KOSTUK, R. K., 1995, J. opt. Soc. Am. A, 12, 1113.
- [20] JACKSON, J. L., and CORIELL, S. R., 1968, Appl. Phys., 39, 2349.
- [21] GRANN, E. B., MOHARAM, M. G., and POMMET, D. A., 1994, J. opt. Soc. Am. A, 11, 2695.
- [22] Brauer, R., and Bryngdahl, A., 1994, Appl. Optics, 33, 7875.
- [23] GRANN, E. B., and MOHARAM, M. G., 1995, OSA Annual Meeting, Portland, September, paper Thhh3.
- [24] Gradshteyn, I. S., and Ryzhik, I. M., 1965, Tables of Integrals Series and Products (New York, San Francisco and London: Academic Press), chapter 1, pp. 38-39.
- [25] Li, L., and Haggans, C. W., 1993, JOSA A, 10, 1184.
- [26] WANG, S. S., MAGNUSSON, R., BAGBY, J. S., and MOHARAM, M. G., 1990, J. opt. Soc. Am. A, 8, 1470.
- [27] NOPONEN, E., and TURUNEN, J., 1994, JOSA A, 11, 2494.
- [28] PENG, S., and Morris, G. M., 1995, J. opt. Soc. Am. A, 12, 1087.